

# 000 UNBIASED VISUAL REASONING WITH CONTROLLED 001 VISUAL INPUTS 002

003 **Anonymous authors**

004 Paper under double-blind review

## 005 ABSTRACT

006 End-to-end Vision-language models (VLMs) often rely on spurious visual cues,  
007 conflating perception with decision-making. We introduce VISTA (Visual Infor-  
008 mation Separation for Text-based Analysis), which enforces an explicit informa-  
009 tion bottleneck between a text-only reasoner and a stateless VLM sensor. The  
010 LLM reasoner decomposes each question and iteratively queries a VLM for vi-  
011 sual facts; the VLM is instructed to reject queries that require high-level infer-  
012 ence, creating an explicit information bottleneck. Trained on only 641 questions,  
013 VISTA yields large robustness gains on SpuriVerse across two vision backbones  
014 (+16.29% with Qwen-2.5-VL-7B and +6.77% with Llama-3.2-Vision-11B), while  
015 direct SFT or RL on the VLM fails to remedy spuriousity and can even exacerbate  
016 it. Despite never exposing the reasoner to raw pixels, VISTA slightly improves or  
017 remains on par with VLMs on everyday-scene benchmarks, including MMVP and  
018 SeedBench. Our learned reasoners transfer across sensors, indicating algorithmic  
019 rather than model-specific generalization. Together, VISTA enables spurious-  
020 resistant VQA by upgrading the brain, not the eyes.

## 021 1 INTRODUCTION

022 Recent advances in vision–language models (VLMs) have propelled multimodal understanding and  
023 visual question answering (VQA) to new heights. However, beneath these impressive benchmarks  
024 lies a persistent concern: many systems appear to succeed not by genuine visual reasoning, but  
025 by exploiting shortcuts that correlate spuriously with the correct answer, including contextual cues,  
026 visual predominance, or commonly co-occurring objects (Yang et al., 2025; Kervadec et al., 2021;  
027 Dancette et al., 2021; Si et al., 2022; Agrawal et al., 2018; Wang et al., 2024a;b; Ye et al., 2024).  
028 An example is illustrated in Figure 1: when asked “are the men assembling parts of a building?”,  
029 the end-to-end Qwen2.5-VL-7B model answers “yes” based on the presence of scaffolding and  
030 stereotypical attire, while failing to verify whether any assembly action is actually taking place.

031 Critically, this conflation of perception and reasoning is problematic not only at inference but also  
032 during training. When a model is trained end-to-end from answers, it is difficult to provide learning  
033 signals that distinguish relevant causal evidence from correlated but irrelevant cues. As a result, end-  
034 to-end training on VLMs can reward the use of shortcuts and entangle visual features with high-level  
035 decision-making, producing brittle behaviors under distribution shift or adversarial perturbations.

036 To address these limitations, we introduce VISTA (Visual-Information Separation for Text-based  
037 Analysis), a new meta-architecture and learning paradigm that enforces an information bottleneck  
038 between perception and reasoning modules. Our key intuition is simple: by restricting the reasoning  
039 module to obtain visual information only through a low-bandwidth, objective query interface, we  
040 reduce the opportunity to exploit spurious correlations, force the reasoner to rely on logical deduc-  
041 tion as well as targeted evidence gathering, and create a clearer credit assignment during training. In  
042 VISTA, raw visual inputs are handled by a frozen VLM that answers simple and objective queries,  
043 while rejecting complex or vague requests. All decision-making occurs in an LLM reasoner that  
044 plans queries, integrates visual evidence, and explains its conclusions step-by-step.

045 As illustrated in Figure 1, VISTA operates as an iterative dialogue between an LLM reasoner and  
046 a VLM sensor constrained to answer simple, objective queries. Given a question, the reasoner  
047 conducts step-wise, verbalized planning and issues targeted visual checks; the sensor either rejects or  
048 returns short factual responses. In the earlier example, our reasoner remains unaffected by spurious

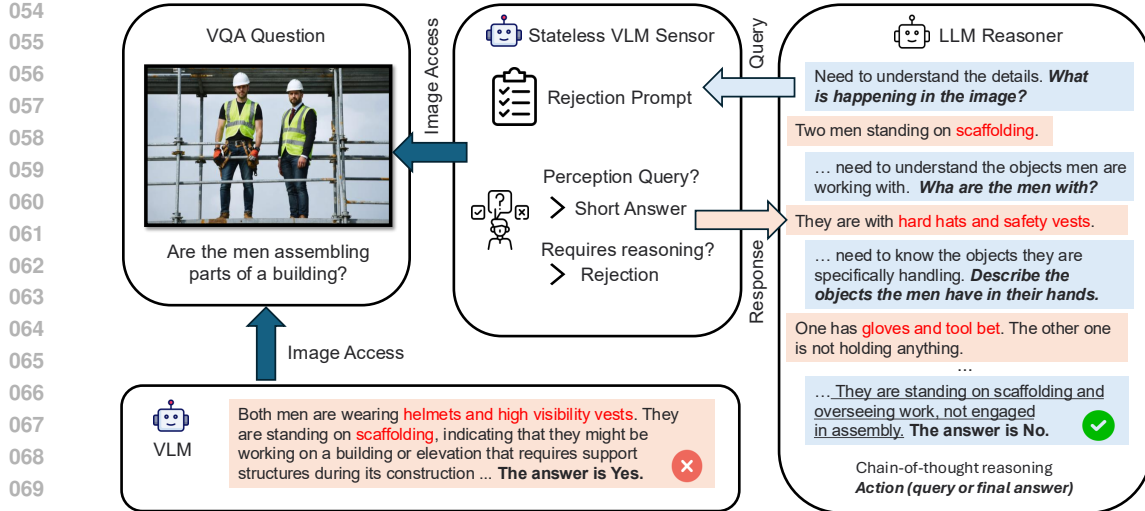


Figure 1: Comparison between an end-to-end VLM and VISTA on a SpuriVerse example (actual model outputs). Spurious attributes are highlighted in red. **Bottom:** The end-to-end Qwen2.5-VL model predicts **Yes** by exploiting spurious attributes (e.g., scaffolding and stereotypical attire) that are irrelevant to the question, resulting in an error. **Top:** VISTA decouples perception from reasoning via an information bottleneck and follows a neutral, iterative decision process: the LLM reasoner emits CoT rationales before each action, issues targeted simple visual queries as actions, and terminates the interaction once a conclusion is reached. By explicitly checking the men’s actions and interactions, the reasoner remains invariant to the spurious cues and correctly predicts **No**.

attributes and explicitly verifies the men’s actions by checking whether they are interacting with any tools or objects indicative of assembly. By pursuing a neutral, evidence-seeking reasoning path, VISTA correctly concludes that the men are standing and overseeing rather than assembling.

We summarize our contributions as follows:

- We propose VISTA, a framework and corresponding learning paradigm that formalizes VQA as an iterative decision-making process under an information bottleneck that separates perception from reasoning.
- We demonstrate that, with the same data and training steps, VISTA encourages neutral, evidence-seeking reasoning across two vision backbones, whereas end-to-end training (SFT and RL) on VLMs reinforces visual shortcuts and reduces robustness.
- VISTA attains substantial robustness gains on Spuriverse while remaining on par with end-to-end systems on everyday-scene benchmarks (MMVP, SeedBench)

## 2 RELATED WORK

**Modular VQA Systems.** Early modular VQA systems explicitly decompose problems into perception and reasoning components. Neural Module Networks dynamically compose modular networks depending on the question structure (Andreas et al., 2016). Neural-Symbolic VQA parses questions into executable programs against structured scene graphs (Yi et al., 2018). These methods separate recognition from symbolic reasoning but often rely on strong supervision or curated representations. Later ViperGPT and VisProg show that LLMs, with strong built-in code generation capabilities, can compose visual operators as programs, offering strong interpretability and compositional generalization (Surís et al., 2023; Gupta & Kembhavi, 2023). Compared with these programmatic modular systems, our formulation uses language as the interface to perception, avoiding coverage gaps and engineering constraints imposed by APIs or program libraries. In addition, our reasoning proceeds iteratively, which supports complex reasoning and produces auditable traces. Crucially, we impose an information bottleneck to mitigate visual biases, which underpins our motivation to encourage neutral visual reasoning. To address limitations from domain-specific decomposition and premature

108 conclusions without sufficient visual information in multi-step VQA, IdealGPT decomposes ques-  
 109 tions into sub-questions and delegates answering to a VLM (You et al., 2023). Our formulation  
 110 shares the same high-level recipe, including LLM-based decomposition and iterative reasoning, but  
 111 differs in fundamental ways: (1) we enforce a perception-only interface that explicitly targets vi-  
 112 sual bias mitigation; (2) we study a training paradigm and compare directly with end-to-end VLM  
 113 training, whereas IdealGPT is evaluated zero-shot with a closed LLM; (3) our method trains a single  
 114 LLM to decompose, reason, and decide the final answer, whereas IdealGPT assumes separate strong  
 115 models (ChatGPT) for questioning and reasoning.

116 **Robustness, Shortcut Learning, and Evaluation Benchmarks.** VQA robustness work shows that  
 117 models often exploit shortcuts rather than genuine reasoning. VQA-CP introduces changing-prior  
 118 splits to break question-type priors and reveals large drops for models under shifted priors (Agrawal  
 119 et al., 2018). Beyond question-only biases, VQA-CE mines multimodal shortcut rules and demon-  
 120 strates that many debiasing methods remain ineffective when the shortcuts are cross-modal (Dancette  
 121 et al., 2021). GQA-OOD reorganizes the GQA dataset and finds that strong VQA models still fail on  
 122 infrequent or shifted compositions (Kervadec et al., 2021). More recently, MM-SpuBench probes  
 123 spurious biases by asking models to pick the diagnostic feature for object identity (Ye et al., 2024).  
 124 Since our claims center on QA accuracy under controlled spurious shifts and reasoning, we consider  
 125 datasets aligned with those goals. SpuriVerse curates real-world VLM failures attributed to spuri-  
 126 ous cues and validates them with synthetic counterfactuals (Yang et al., 2025). In parallel, MMVP  
 127 targets basic visual-pattern failures and SEED-Bench provides broad, human-annotated multiple-  
 128 choice evaluations and enables standardized comparison across models (Tong et al., 2024; Li et al.,  
 129 2023; 2024). Our approach is complementary to dataset-level and loss-level debiasing: instead of  
 130 reweighting data or adding regularizers, we enforce an architectural bottleneck that promotes neutral  
 131 visual reasoning while remaining compatible with everyday suites and spurious-stress evaluations.

132 **Active Reasoning and Reinforcement Learning.** Active information-seeking has been studied in  
 133 multi-hop QA and fact verification (Yang et al., 2018; Thorne et al., 2018) as well as in interactive  
 134 environments (Shridhar et al., 2020; Yao et al., 2022; Zhou et al., 2023). LLM agents often alter-  
 135 nate between planning, tool use, and verification, sometimes under explicit budgets. Foundational  
 136 systems interleave reasoning with actions (Yao et al., 2023), browse and cite sources with human  
 137 feedback (Nakano et al., 2021), and improve over trials via self-reflection (Shinn et al., 2023). Our  
 138 setting shares the multi-turn nature but differs in objective: rather than maximizing task success by  
 139 any means, we explicitly constrain how information can be acquired to prevent shortcut learning.

140 On learning signals, RL has been effective for aligning multi-turn behaviors and tool use. Popular  
 141 training paradigms include PPO-based RLHF with KL control for long-horizon tool use and dialogue  
 142 (Nakano et al., 2021; Ouyang et al., 2022), AI-feedback variants that reduce human labeling (Bai  
 143 et al., 2022; Lee et al., 2023), and offline preference optimization (Rafailov et al., 2023). Recent  
 144 group-based objectives (GRPO) stabilize reasoning-centric training by scoring multiple completions  
 145 per prompt and using relative advantages (Shao et al., 2024). Our setting is algorithm-agnostic, and  
 146 we adopt GRPO for its practicality and strong uptake in reasoning-focused LLMs.

### 147 3 METHOD

#### 149 3.1 OVERVIEW

151 We decompose a VQA system into a text-only **reasoner**  $\pi_\theta$ , and a frozen VLM **sensor**  $S_\phi$  that  
 152 answers perception-only questions. Given the textual input question  $q$ , the reasoner iteratively inter-  
 153 acts with the sensor by issuing free-form natural-language queries; the sensor sees the input image  
 154  $x$ , and either returns a short answer or rejects the query when it requires high-level inference. The  
 155 interaction loop terminates when the reasoner concludes with an answer or the maximum number of  
 156 steps is reached.

157 Formally, at step  $t$ , the reasoner observes the conversation history

$$158 \quad 159 \quad h_t = (q, (s_1, y_1), \dots, (s_{t-1}, y_{t-1})),$$

160 where  $s_i$  and  $y_i$  are the output strings of  $\pi_\theta$  and  $S_\phi$  at step  $i$ . Each  $s_t$  contains two parts:

161 

- Chain-of-thought  $c_t$ : text used by the reasoner to think before outputting an action

162

**Algorithm 1** VISTA reasoning loop

163

```

Require: image  $x$ , question  $q$ , reasoner  $\pi_\theta$ , sensor  $S_\phi$ , step budget  $T_{\max}$ 
1:  $h \leftarrow [q]$  ▷ Reasoner history of pairs  $(s_i, y_i)$ 
2: for  $t = 1$  to  $T_{\max}$  do
3:    $s_t \sim \pi_\theta(\cdot \mid h)$  ▷ Reasoner raw text at step  $t$ 
4:   parse  $s_t \rightarrow (c_t, u_t)$ 
5:   if  $u_t = \text{ANSWER}(a_t)$  then
6:     return  $a_t$  ▷ Terminate upon answer
7:   else if  $u_t = \text{QUERY}(q_t)$  then
8:      $y_t \leftarrow S_\phi(x, q_t)$  ▷ Sensor sees only  $(x, q_t)$ ; no  $q$ , options, or history
9:      $h \leftarrow h \parallel (s_t, y_t)$  ▷ Append  $(s_t, y_t)$  to history
10:  end if
11: end for
12: return  $s_t$ 

```

164

165

166

167

168

169

170

171

172

173

174

175

176

177

178

179

180

181

182

183

184

185

186

187

188

189

190

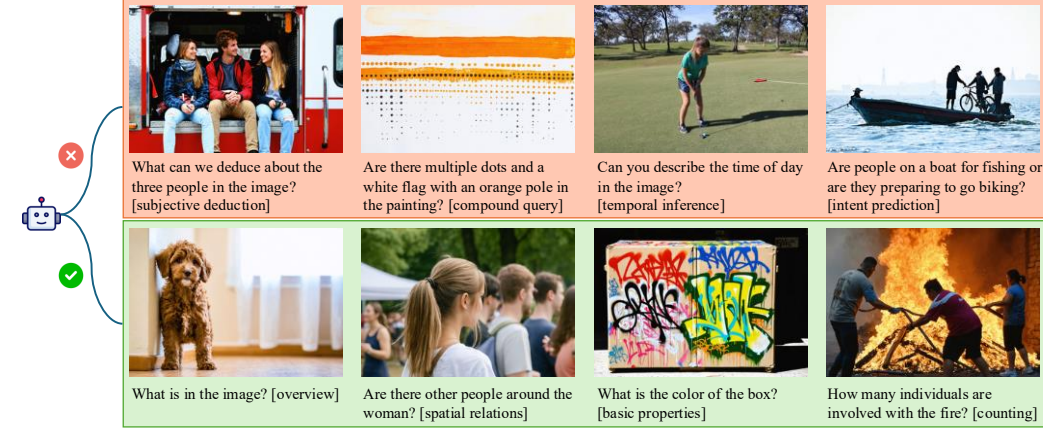


Figure 2: **Accepted vs. rejected queries.** The top row shows rejected cases, and the bottom row shows accepted cases. The vision-only *sensor* answers perception questions in six categories and may emit one brief *OVERVIEW* when the text is under-specified; all requests requiring high-level inference are **REJECTED**. Top Row is rejected, below row is accepted

191

192

193

194

195

196

197

- Action  $u_t$ : a structured directive extracted with a deterministic rule-based parser

198

The reasoner implicitly learns to decide *what to ask* and *when to stop*. The action space is

199

200

$$u_t \in \mathcal{U} = \{\text{QUERY}(q_t), \text{ANSWER}(a_t)\},$$

201

202

where  $q_t$  is a query string and  $a_t$  is a final answer string. The loop terminates if a final answer is extracted; otherwise, the sensor receives  $q_t$  and returns

203

204

$$y_t = S_\phi(x, q_t).$$

205

206

207

208

Crucially, the stateless sensor  $S_\phi$  never receives the history or the reasoning traces; it only sees the contextless query  $q_t$  and image  $x$ . Thus, all task-level decision-making must arise from  $\pi_\theta$ . The working pipeline of VISTA is illustrated in Algorithm 1.

209

210

### 3.2 PERCEPTION-ONLY QUERIES AND REJECTION POLICY

211

212

213

214

215

We decompose the system into a text-only *reasoner*  $\pi_\theta$  and a vision-only *sensor*  $S_\phi$ . Following the taxonomy of perception question of Selvaraju et al. (2020), the sensor answers free-form *perception* queries limited to: *Existence* (“Is there a bicycle?”), *Basic Properties* (“Is the mug red?”), *Spatial Relations* (“What is left of the sofa?”), *Simple Activities* (“Are they looking at the camera?”), *Text/Symbol Recognition* (“What does the road sign say?”), and *Counting* (“How many cups are on the table?”).

216 **Objective overview (optional).** When a question lacks sufficient textual context, the sensor may  
 217 provide a brief, objective *overview* of the scene (one short sentence; perception-only). The overview  
 218 supplies minimal global context (scene type, dominant objects with coarse counts, coarse layout,  
 219 basic global attributes) to reduce referential uncertainty and establish a stable spatial frame before  
 220 targeted follow-ups. It explicitly excludes intentions, causes, roles, emotions, events beyond static  
 221 poses, and any world knowledge.

222 **Rejection policy and enforcement.** Any request that requires high-level inference or remains  
 223 ambiguous beyond what an objective overview can resolve needs to be rejected by outputting a  
 224 fixed template “I cannot answer this question.” Concretely, we reject queries involving multi-hop or  
 225 causal reasoning, reliance on external knowledge, subjective interpretation beyond what is directly  
 226 observable, or prompts that should be decomposed into simpler perception primitives. We *enforce*  
 227 this behavior with an explicit accept/reject instruction prompt and response format. Examples of  
 228 accepted/rejected queries are shown in Fig. 2, and the full prompt is provided in Appx. H. Human  
 229 analysis (Section 7.3) of 100 randomly sampled cases shows 86% agreement with human pass/reject  
 230 labels, evidencing an effective rejection policy.

### 232 3.3 REINFORCEMENT LEARNING REASONER

233 Our learning strategy formulates VQA solving as a sequential decision-making process and provides  
 234 the reasoner with an explorable environment with clear reward signals, making RL training a well-  
 235 suited choice. We optimize  $\pi_\theta$  using Group Relative Policy Optimization (GRPO) (Shao et al.,  
 236 2024). Each episode  $\tau$  yields a terminal reward based on final answer correctness:

$$237 R(\tau) = \mathbb{1}[a_T = a^*]. \quad (1)$$

238 Training differs from single-step GRPO only in the sampling of rollouts and the assignment of  
 239 loss masks. We apply the GRPO update to the union of *assistant-only* tokens across all assistant  
 240 turns. With terminal-only reward and unit discount, the group-relative advantage is constant within  
 241 a trajectory, so the update is effectively the single-step GRPO objective applied to a longer, state-  
 242 dependent sequence (details in App. B).

## 245 4 THEORETICAL ANALYSIS

246 Intuitively, overfitting thrives when the learner can absorb rich, high-variance signals and latch onto  
 247 spurious correlations that happen to predict labels in the training set. By constraining the visual  
 248 bandwidth, we shrink the hypothesis space the reasoner can realize: high-level, shortcut features  
 249 cannot pass through the interface, forcing predictions to rest on a small set of stable, perception-  
 250 level facts. In this section, we formalize this intuition by relating generalization to the information  
 251 that can flow through the sensor–reasoner interface.

252 **Setup.** Let  $(X, Q, Y) \sim D$  denote image, question, label. A reasoner interacts with a sensor for at  
 253 most  $T$  steps. At step  $t$ , the reasoner emits a free-form text query  $a_t$ ; the sensor enforces a rejection  
 254 rule  $R_t = g(a_t) \in \{0, 1\}$ : if  $R_t = 0$ , it turns a rejection template  $\perp$ ; otherwise it returns a short per-  
 255 ception answer from a finite alphabet  $O_t \in \Sigma$ . Let  $Z_{1:T} = (Z_1, \dots, Z_T)$ ,  $Z_t \in \Sigma_\perp := \Sigma \cup \{\perp\}$  be  
 256 the visual evidence. We train parameters  $W$  from the compressed dataset  $\tilde{D} = \{(Z_{1:T}, Q_i, Y_i)\}_{i=1}^n$ .  
 257 We assume the learning loss  $\ell(W; Z, Q, Y) \in [0, 1]$  is bounded. The true loss and empirical loss are  
 258 defined as  $L(W) = \mathbb{E}\ell(W; Z, Q, Y)$  and  $\hat{L}(W, \tilde{D}) = \frac{1}{n} \sum_{i=1}^n \ell(W; Z_i, Q_i, Y_i)$ .

259 **Theorem** (Informal, generalization under an information bottleneck).

$$260 |\mathbb{E}[\hat{L}(W, \tilde{D}) - L(W)]| \leq \sqrt{2C_T},$$

261 where  $C_T$  is the per-example bit budget

$$262 C_T := T \log |\Sigma_\perp|$$

263 **Implications and Limitations.** The expected generalization gap depends only on the interface  
 264 budget  $C_T$  and is independent of the size of the training data, where a smaller  $C_T$  means less  
 265 overfitting. While the bound captures average generalization, it does not alone guarantee worst-case  
 266 adversarial robustness nor account for distribution shift without extra assumptions. The complete  
 267 proof is included in Appendix A.

270 

## 5 EXPERIMENT SETUP

271 

### 5.1 DATASETS AND PREPROCESSING

272 We evaluate on three benchmarks with no overlap with questions in the training set: SpuriVerse  
 273 (Yang et al., 2025), MMVP (Tong et al., 2024), and SeedBench (Li et al., 2023). SpuriVerse consists  
 274 of 1200 questions explicitly constructed around real-world spurious correlations, making it well-  
 275 suited for testing reasoning robustness under adversarial conditions. MMVP stresses perceptual  
 276 limitations by constructing CLIP-blind image pairs and associated questions that expose visual-  
 277 grounding failures. SeedBench is for everyday, non-adversarial performance, due to its scale, we  
 278 randomly sample 500 single-image questions to keep the compute and time tractable. Because in  
 279 SpuriVerse more than 60% of gold answers appear in option B, we mitigate answer-position bias  
 280 by shuffling the multiple-choice options. Shuffling is applied once as a deterministic pre-processing  
 281 step, and the exact same shuffled inputs are used across all evaluation settings. We report both the  
 282 original and shuffled results in Appendix C and observe that our method consistently outperforms  
 283 all baselines and yields significant improvements. We present the shuffled results in the main text,  
 284 as they remove label-position bias while preserving the overall trend.

285 

### 5.2 VISTA AND BASELINE SETTINGS

286 **VISTA.** For all experiments, we use Qwen2.5-7B as the LLM reasoner. We train and instantiate our  
 287 method with two frozen VLM sensors: Qwen2.5-VL-7B and Llama3.2-11B. For each sensor, we  
 288 evaluate three settings: (i) VISTA (base): with an untrained reasoner (reference model) interacting  
 289 with the sensor; and (ii) VISTA (RL): with trained reasoner using GRPO.

290 **Baselines.** We compare against end-to-end VLMs using the same two backbones in the following  
 291 settings: (i) E2E (base): the untrained VLM directly answers the question; (ii) E2E (base + CoT): the  
 292 untrained VLM outputs chain-of-thoughts before answers; (iii) E2E (SFT): supervised fine-tuning  
 293 to directly answer; and (iv) E2E (RL): we additionally evaluate a GRPO-trained Qwen2.5-VL-7B  
 294 on the same training data and for the same number of steps as VISTA (RL). These baselines isolate  
 295 where gains come from our framework design and training signals.

296 

### 5.3 EVALUATION PROTOCOLS

297 We report accuracy on SpuriVerse, MMVP, and SeedBench-500. For a fair comparison, we stan-  
 298 dardize sampling and decoding across methods: both VISTA and end-to-end VLMs use 11-sample  
 299 self-consistency at temperature 1.0 for the *predictive component* (the LLM reasoner in VISTA and  
 300 the VLM itself in end-to-end baselines), and the majority-voted answers are evaluated. For VISTA,  
 301 the reasoner–sensor interaction is capped at  $T_{\max} = 24$  and the LLM reasoner is sampled at tem-  
 302 perature 1.0, while the VLM sensor’s temperature is set to 0 during both training and evaluation.  
 303 Because end-to-end VLMs may emit unparsable multiple-choice strings, we canonicalize raw out-  
 304 puts to the option set with a lightweight Qwen-2.5-7B post-processor prior to evaluation.

305 

### 5.4 TRAINING SETUP

306 We construct the training set by sampling questions from five sources: VQAv2 (Goyal et al., 2017),  
 307 Visual7W (Zhu et al., 2016), GQA (Ainslie et al., 2023), A-OKVQA (Schwenk et al., 2022), and  
 308 VQA-Introspect (Selvaraju et al., 2020). We then apply a multi-stage filtering pipeline that (1)  
 309 retains questions likely to elicit multi-step reasoning and (2) removes examples solvable via easy  
 310 visual or textual shortcuts. This yields a training split of 641 questions (A-OKVQA: 502, VQA-  
 311 Introspect: 95, Visual7W: 34, VQAv2: 7, GQA: 3). Details of the filtering process and the resulting  
 312 composition are summarized in Appendix D. We provide details of RL and SFT training in the  
 313 Appendix E.

314 

## 6 MAIN RESULTS

315 We present our main results in Table 1. We report accuracy on SpuriVerse, MMVP and SeedBench-  
 316 500. For each vision backbone, we show the  $\Delta$  relative to its corresponding E2E (base); positive

324  
325  
326 Table 1: Main results on SpuriVerse, MMVP and SeedBench-500.  
327  
328  
329  
330  
331  
332  
333  
334  
335  
336  
337  
338  
339  
340  
341  
342  
343  
344  
345  
346  
347  
348  
349  
350  
351  
352  
353  
354  
355  
356  
357  
358  
359  
360  
361  
362  
363  
364  
365  
366  
367  
368  
369  
370  
371  
372  
373  
374  
375  
376  
377

VLM	Setting	SpuriVerse	Δ	MMVP	Δ	SeedBench-500	Δ
Qwen2.5-VL	E2E (base)	37.50		51.33		71.20	
	E2E (base + CoT)	47.42	+9.92	52.67	+1.34	<b>73.20</b>	+2.00
	E2E (SFT)	34.84	-2.66	50.67	-0.66	72.40	+1.20
	E2E (RL)	44.52	+7.02	<b>53.33</b>	+2.00	73.00	+1.80
	VISTA (base)	46.29	+8.79	46.67	-4.66	66.80	-4.40
	VISTA (RL)	<b>53.79</b>	+16.29	50.00	-1.33	71.60	+0.40
Llama3.2-Vision	E2E (base)	39.76		45.33		72.20	
	E2E (base + CoT)	38.87	-0.89	48.00	+2.67	<b>73.20</b>	+1.00
	E2E (SFT)	40.16	+0.40	32.00	-13.33	66.80	-5.40
	VISTA (base)	44.44	+4.68	35.33	-10.00	68.80	-3.40
	VISTA (RL)	<b>46.53</b>	+6.77	<b>52.67</b>	+7.34	71.80	-0.40

changes are highlighted in green and drops in red. The best numbers for each dataset and backbone are bolded.

**Robustness to spurious correlations.** We evaluate on SpuriVerse, which is based on real-world spurious cues, and compare our approach with E2E VLM baselines under an identical evaluation protocol. In the inference-only setting (VISTA base in the table), we use an untrained LLM paired with a frozen VLM sensor and our results already match or surpass the best performing E2E systems. with Qwen2.5-VL as the sensor, VISTA scores 46.29%, approaching the best E2E baseline (untrained + CoT) at 47.42%; with Llama-3.2-Vision, VISTA reaches 44.44%, outperforming the best E2E baseline (SFT) at 40.16%. These results support our design that constraining the interface to perception-only queries keeps the reasoner on a neutral, evidence-seeking path rather than following spurious visual shortcuts, and the gains hold model-agnostically across sensors. With RL-trained reasoners (sensors remain frozen), performance further improves and the gaps widen. On Qwen2.5-VL, RL yields a 7.5% improvement over our base policy to 53.79%, extending the margin over the best E2E baseline to 6.37%; on Llama-3.2-Vision, RL attains 46.53% and maintains a 6.37% lead over the strongest E2E (SFT) baseline. Additionally, We provide a manual analysis that further confirms our improvements stem from a more neutral and evidence-linked reasoning process. Details are in Section 7.3.

**General performance on MMVP and SeedBench.** To contextualize robustness results, we evaluate on MMVP and SeedBench-500, targeting everyday-scene questions whose answers can be inferred from a small set of observable visual predicates combined with commonsense and short multi-step reasoning. Overall, VISTA delivers substantial robustness gains with only marginal accuracy trade-offs relative to the strongest E2E baselines. On MMVP, our RL-trained reasoner improves over the strongest E2E baseline with Llama3.2-Vision (52.67% vs. 48.00%) and is only marginal behind the strongest baselines with Qwen2.5-VL by 3.33%. SeedBench provides a general and non-adversarial testbed, and our results are slightly below the best E2E baselines (Qwen2.5-VL: 71.60% vs. 73.20%; Llama3.2-Vision: 71.80% vs. 73.20%). Because SeedBench does not target adversarial spuriousness, end-to-end VLMs with raw-pixel access can exploit benign correlations and holistic cues, yielding a small but consistent edge. By contrast, our architecture enforces a perception-only interface that promotes neutral, evidence-based reasoning under constrained visual bandwidth, introducing an explicit trade-off between information bandwidth and neutrality. The rejection ablation in Section 7.1 supports this hypothesis, and we approach E2E results when the rejection bottleneck is removed.

**Comparison of learning strategies.** We compare SFT and RL applied either to end-to-end VLMs or to our reasoner in VISTA, using the same training data and schedule. In this section, we compare and report the improvement gains of the trained model compared with its base policy. For example, E2E SFT baselines are measured against E2E base (no CoT), while E2E RL are measured against E2E base + CoT; VISTA deltas are measured against their own base policy. Across both vision backbones, training VISTA yields consistent, sizable gains over its base, whereas training the VLM end-to-end produces marginal and often inconsistent improvements. The effect is most pronounced

378 Table 2: Ablation on the VLM rejection bottleneck with Metrics: acc = accuracy, rnd = average  
 379 conversations rounds, rej = rejection rate.

381 <b>VLM</b>	382 <b>Setting</b>	383 <b>SpuriVerse</b>			384 <b>SeedBench-500</b>		
		385 <b>acc</b>	386 <b>rnd</b>	387 <b>rej</b>	388 <b>acc</b>	389 <b>rnd</b>	390 <b>rej</b>
391 Qwen2.5-VL	392 VISTA (base), w/ rejection	<b>46.29</b>	3.38	0.18	66.80	3.43	0.20
	393 VISTA (base), w/o rejection	43.23	3.05	0.00	<b>69.40</b>	3.03	0.00
	394 VISTA (RL), w/ rejection	<b>53.79</b>	7.31	0.32	71.60	6.58	0.29
	395 VISTA (RL), w/o rejection	51.37	6.00	0.00	<b>72.80</b>	5.42	0.00

396 on SpuriVerse: all E2E training hurts robustness (Qwen2.5-VL: SFT -2.66%; RL -2.90%; Llama3.2  
 397 SFT has a -0.89% difference), while VISTA-RL improves markedly (+7.5% with Qwen2.5-VL;  
 398 +2.09% with Llama3.2-Vision). On MMVP and SeedBench-500, E2E training yields at best small  
 399 gains, despite becoming more susceptible to spurious cues as evidenced by the SpuriVerse results.  
 400 Taken together, these findings indicate that conflating perception and reasoning during E2E training  
 401 blurs learning signals between causal evidence and correlated but irrelevant features, whereas  
 402 VISTA’s perception-only interface creates a better-suited learning environment in which RL can  
 403 reliably shape neutral, evidence-seeking policies.

## 404 7 ANALYSIS AND DISCUSSIONS

### 405 7.1 REJECTION ABLATION

406 We ablate the rejection bottleneck and investigate its effect in two regimes: adversarial spurious  
 407 correlations (SpuriVerse) and non-adversarial everyday scenes (SeedBench). The results reveal a  
 408 clear information-bandwidth-neutrality trade-off. With rejection on, the sensor denies high-level  
 409 inferences and answers only perception-level queries, shifting the burden to the LLM and encour-  
 410 aging evidence-based reasoning under reduced visual bandwidth. With rejection off, the sensor  
 411 answers high-level queries, increasing bandwidth but exposing the system to shortcut exploitation.  
 412 Table 2 reports accuracy alongside mean conversation rounds and rejection rates for VISTA (base)  
 413 and VISTA (RL) with/without rejection. Enforcing the bottleneck improves robustness on Spuri-  
 414 Verse, confirming its value for shielding against spurious cues; removing the bottleneck improves  
 415 SeedBench performance, shortens interactions (fewer rounds), and drives the rejection rate to zero.  
 416 Notably, the RL variant without rejection attains near-parity with the strongest E2E baseline on  
 417 SeedBench, suggesting that relaxing the gate can recover benign, non-adversarial cues while the full  
 418 bottleneck remains preferable under adversarial conditions. Our results also indicate that RL training  
 419 promotes deeper evidence-seeking, as evidenced by an increase in the average number of conver-  
 420 sation rounds. As future work, we will investigate rejection-aware, efficiency-regularized learning  
 421 to induce more concise reasoning and develop adaptive, confidence-aware gating that modulates  
 422 rejection to balance information bandwidth and neutrality.

### 423 7.2 ZERO-SHOT GENERALIZATION ON UNSEEN VLM SENSOR

424 To test whether the policy exploits VLM-specific patterns, we perform a zero-shot sensor swap:  
 425 the reasoner trained with a Qwen2.5-VL sensor is paired with an unseen Gemma3 sensor. Without  
 426 any additional tuning, it remains strong and consistently outperforms all untrained end-to-end VLM  
 427 baselines, indicating sensor-agnostic reasoning. The results are summarized in Table 3.

### 428 7.3 MANUAL ANALYSIS

429 To complement our quantitative benchmarks and capture qualitative aspects of reasoning that au-  
 430 tomated metrics miss, we conducted a three-part human evaluation. We recruited four expert an-  
 431 notators with complementary backgrounds and a specialist in vision-language modeling to provide  
 432 independent judgments. For each question, two annotators provided independent labels, and the

432 Table 3: Zero-shot results of learned VISTA reasoner paired with unseen vision models (replacing  
 433 Qwen2.5-VL with Gemma3-12B).

VLM	Setting	SpuriVerse	MMVP	SeedBench-500
Gemma3	E2E (base)	33.63	46.00	66.40
	E2E (base + CoT)	38.87	44.67	67.00
	VISTA (base)	37.74	38.66	64.40
	VISTA (RL, Zero-shot)	<b>43.87</b>	<b>50.67</b>	<b>67.80</b>

441  
 442 specialist audited rater quality and resolved disagreements. Detailed annotation materials, including  
 443 the presented item, evaluation prompt, response options, and guidance, are provided in Appendix I.

444 **Reasoning Neutrality.** We conducted a manual audit of a random sample of 30 SpuriVerse ques-  
 445 tions, evaluating VISTA RL traces against end-to-end Chain-of-Thought (E2E-CoT) traces. In this  
 446 task, 76.67% of VISTA traces did not rely on spurious attributes, compared with 43.33% for E2E,  
 447 suggesting that blind reasoning is less affected by spurious cues. Detailed instructions and prompt  
 448 templates appear in Appendix 8, a representative example is shown in Figure 3.

449 **Error Analysis.** We conducted a focused human study of error diagnosis using 100 question-answer  
 450 pairs from SpuriVerse, MMVP, and SeedBench-500 whose final answers were incorrect, together  
 451 with their VISTA RL traces. Overall, 56% of errors were attributed to the VLM (incorrect percep-  
 452 tion or inappropriate rejection), 28% to the LLM (option misalignment, guessing, or logical error),  
 453 and 13% to other factors (rounding explains the remainder), indicating that most failures originate  
 454 in the vision module. The complete rubric and prompt templates are provided in Appendix 9, and  
 455 Figure 3 presents a worked example.

456 **Rejection Behavior Alignment:** To evaluate the rejection filter, we randomly sampled 100 decom-  
 457 posed question-answer pairs from the VISTA RL dialogues across the three datasets and compared  
 458 the VLM’s pass/reject decisions with human-annotated gold labels. We report precision, recall, and  
 459 F1 under positive class conventions. Treating pass as positive yields precision = 86.0%, recall =  
 460 92.96%, and F1 = 88%. These results indicate good alignment with human labels on pass and rejec-  
 461 tion decisions. Appendix 10 provides the complete instructions and prompt templates, and Figure 5  
 462 presents a concrete example.

#### 463 7.4 ADDITIONAL ANALYSIS

464 We report two complementary studies in Appendix F. **(i) Reasoner transfer.** We additionally test  
 465 whether the reasoner overfits to a specific VLM by swapping the paired sensors at evaluation time  
 466 between Qwen2.5-VL and Llama-3.2 (Appendix F.1). The main trends persist: even under sen-  
 467 sor swap, the reasoner remains competitive compared with E2E baselines. **(ii) VISTA training**  
 468 **ablation.** We compare SFT against RL for training the VISTA reasoner and find that disillation  
 469 from successful trajectories alone does not yield a reliably generalizable policy, underscoring the  
 470 importance of framing VISTA as an RL problem (Appendix F.2).

## 471 8 CONCLUSION

472 We introduced VISTA, a modular framework that enforces an explicit information bottleneck be-  
 473 tween perception and reasoning. A text-only reasoner interacts with a stateless visual sensor that  
 474 answers only perception-level queries or rejects high-level ones, thereby separating decision making  
 475 from raw visual features and improving credit assignment. This design yields a learning environ-  
 476 ment that naturally encourages evidence-seeking and neutral reasoning, in contrast to end-to-end  
 477 SFT/RL pipelines that tend to entangle spurious visual cues with downstream predictions.

478 Empirically, VISTA delivers consistent gains in robustness on adversarial, spurious-correlation  
 479 settings while remaining competitive on everyday-scene benchmarks. Policies learned under our  
 480 framework transfer across vision backbones and unseen sensors, indicating cross-model generaliza-  
 481 tion rather than model-specific overfitting. Ablations of the rejection mechanism reveal a measured

486 bandwidth–neutrality trade-off: tighter interfaces suppress shortcut use but restrict high-level inference,  
 487 whereas looser interfaces increase capacity at the risk of bias exploitation.  
 488

489 **REFERENCES**

491 Aishwarya Agrawal, Dhruv Batra, Devi Parikh, and Aniruddha Kembhavi. Don’t just assume;  
 492 look and answer: Overcoming priors for visual question answering. In *Proceedings of the IEEE*  
 493 *conference on computer vision and pattern recognition*, pp. 4971–4980, 2018.

494 Joshua Ainslie, James Lee-Thorp, Michiel De Jong, Yury Zemlyanskiy, Federico Lebrón, and Sumit  
 495 Sanghai. Gqa: Training generalized multi-query transformer models from multi-head check-  
 496 points. *arXiv preprint arXiv:2305.13245*, 2023.

497 Jacob Andreas, Marcus Rohrbach, Trevor Darrell, and Dan Klein. Neural module networks. In  
 498 *Proceedings of the IEEE Conference on Computer Vision and Pattern Recognition (CVPR)*, June  
 499 2016.

500 Yuntao Bai, Saurav Kadavath, Sandipan Kundu, Amanda Askell, Jackson Kernion, Andy Jones,  
 501 Anna Chen, Anna Goldie, Azalia Mirhoseini, Cameron McKinnon, et al. Constitutional ai: Harm-  
 502 lessness from ai feedback. *arXiv preprint arXiv:2212.08073*, 2022.

503 Corentin Dancette, Remi Cadene, Damien Teney, and Matthieu Cord. Beyond question-based bi-  
 504 ases: Assessing multimodal shortcut learning in visual question answering. In *Proceedings of the*  
 505 *IEEE/CVF International Conference on Computer Vision*, pp. 1574–1583, 2021.

506 Yash Goyal, Tejas Khot, Douglas Summers-Stay, Dhruv Batra, and Devi Parikh. Making the v in vqa  
 507 matter: Elevating the role of image understanding in visual question answering. In *Proceedings*  
 508 *of the IEEE conference on computer vision and pattern recognition*, pp. 6904–6913, 2017.

509 Tanmay Gupta and Aniruddha Kembhavi. Visual programming: Compositional visual reasoning  
 510 without training. In *Proceedings of the IEEE/CVF conference on computer vision and pattern*  
 511 *recognition*, pp. 14953–14962, 2023.

512 Corentin Kervadec, Grigory Antipov, Moez Baccouche, and Christian Wolf. Roses are red, violets  
 513 are blue... but should vqa expect them to? In *Proceedings of the IEEE/CVF Conference on*  
 514 *Computer Vision and Pattern Recognition*, pp. 2776–2785, 2021.

515 Harrison Lee, Samrat Phatale, Hassan Mansoor, Kellie Ren Lu, Thomas Mesnard, Johan Ferret,  
 516 Colton Bishop, Ethan Hall, Victor Carbune, and Abhinav Rastogi. Rlaif: Scaling reinforcement  
 517 learning from human feedback with ai feedback. 2023.

518 Bohao Li, Rui Wang, Guangzhi Wang, Yuying Ge, Yixiao Ge, and Ying Shan. Seed-bench: Bench-  
 519 marking multimodal llms with generative comprehension. *arXiv preprint arXiv:2307.16125*,  
 520 2023.

521 Bohao Li, Yuying Ge, Yixiao Ge, Guangzhi Wang, Rui Wang, Ruimao Zhang, and Ying Shan.  
 522 Seed-bench: Benchmarking multimodal large language models. In *Proceedings of the IEEE/CVF*  
 523 *Conference on Computer Vision and Pattern Recognition*, pp. 13299–13308, 2024.

524 Reiichiro Nakano, Jacob Hilton, Suchir Balaji, Jeff Wu, Long Ouyang, Christina Kim, Christo-  
 525 pher Hesse, Shantanu Jain, Vineet Kosaraju, William Saunders, et al. Webgpt: Browser-assisted  
 526 question-answering with human feedback. *arXiv preprint arXiv:2112.09332*, 2021.

527 Long Ouyang, Jeffrey Wu, Xu Jiang, Diogo Almeida, Carroll Wainwright, Pamela Mishkin, Chong  
 528 Zhang, Sandhini Agarwal, Katarina Slama, Alex Ray, et al. Training language models to fol-  
 529 low instructions with human feedback. *Advances in neural information processing systems*, 35:  
 530 27730–27744, 2022.

531 Rafael Rafailov, Archit Sharma, Eric Mitchell, Christopher D Manning, Stefano Ermon, and Chelsea  
 532 Finn. Direct preference optimization: Your language model is secretly a reward model. *Advances*  
 533 *in neural information processing systems*, 36:53728–53741, 2023.

540 Dustin Schwenk, Apoorv Khandelwal, Christopher Clark, Kenneth Marino, and Roozbeh Mottaghi.  
 541 A-okvqa: A benchmark for visual question answering using world knowledge. In *European*  
 542 *conference on computer vision*, pp. 146–162. Springer, 2022.

543 Ramprasaath R. Selvaraju, Purva Tendulkar, Devi Parikh, Eric Horvitz, Marco Tulio Ribeiro, Be-  
 544 smira Nushi, and Ece Kamar. Squinting at vqa models: Introspecting vqa models with sub-  
 545 questions. In *Proceedings of the IEEE/CVF Conference on Computer Vision and Pattern Recog-  
 546 nition (CVPR)*, June 2020.

547 Zhihong Shao, Peiyi Wang, Qihao Zhu, Runxin Xu, Junxiao Song, Xiao Bi, Haowei Zhang,  
 548 Mingchuan Zhang, YK Li, Y Wu, et al. Deepseekmath: Pushing the limits of mathematical  
 549 reasoning in open language models. *arXiv preprint arXiv:2402.03300*, 2024.

550 Noah Shinn, Federico Cassano, Ashwin Gopinath, Karthik Narasimhan, and Shunyu Yao. Reflexion:  
 551 Language agents with verbal reinforcement learning. *Advances in Neural Information Processing  
 552 Systems*, 36:8634–8652, 2023.

553 Mohit Shridhar, Xingdi Yuan, Marc-Alexandre Côté, Yonatan Bisk, Adam Trischler, and Matthew  
 554 Hausknecht. Alfworld: Aligning text and embodied environments for interactive learning. *arXiv  
 555 preprint arXiv:2010.03768*, 2020.

556 Qingyi Si, Fandong Meng, Mingyu Zheng, Zheng Lin, Yuanxin Liu, Peng Fu, Yanan Cao, Weip-  
 557 ing Wang, and Jie Zhou. Language prior is not the only shortcut: A benchmark for short-  
 558 cut learning in VQA. In Yoav Goldberg, Zornitsa Kozareva, and Yue Zhang (eds.), *Find-  
 559 ings of the Association for Computational Linguistics: EMNLP 2022*, pp. 3698–3712, Abu  
 560 Dhabi, United Arab Emirates, December 2022. Association for Computational Linguistics.  
 561 doi: 10.18653/v1/2022.findings-emnlp.271. URL [https://aclanthology.org/2022.  
 562 findings-emnlp.271/](https://aclanthology.org/2022.findings-emnlp.271/).

563 Thomas Steinke and Lydia Zakynthinou. Reasoning about generalization via conditional mutual  
 564 information. In *Conference on Learning Theory*, pp. 3437–3452. PMLR, 2020.

565 Dídac Surís, Sachit Menon, and Carl Vondrick. Vipergpt: Visual inference via python execution  
 566 for reasoning. In *Proceedings of the IEEE/CVF international conference on computer vision*, pp.  
 567 11888–11898, 2023.

568 James Thorne, Andreas Vlachos, Christos Christodoulopoulos, and Arpit Mittal. Fever: a large-scale  
 569 dataset for fact extraction and verification. *arXiv preprint arXiv:1803.05355*, 2018.

570 Shengbang Tong, Zhuang Liu, Yuexiang Zhai, Yi Ma, Yann LeCun, and Saining Xie. Eyes wide  
 571 shut? exploring the visual shortcomings of multimodal llms. In *Proceedings of the IEEE/CVF  
 572 Conference on Computer Vision and Pattern Recognition*, pp. 9568–9578, 2024.

573 Fei Wang, Xingyu Fu, James Y Huang, Zekun Li, Qin Liu, Xiaogeng Liu, Mingyu Derek Ma, Nan  
 574 Xu, Wenzuan Zhou, Kai Zhang, et al. Muirbench: A comprehensive benchmark for robust multi-  
 575 image understanding. In *The Thirteenth International Conference on Learning Representations*,  
 576 2024a.

577 Fei Wang, Wenzuan Zhou, James Y Huang, Nan Xu, Sheng Zhang, Hoifung Poon, and Muahao  
 578 Chen. mdpo: Conditional preference optimization for multimodal large language models. In  
 579 *Proceedings of the 2024 Conference on Empirical Methods in Natural Language Processing*, pp.  
 580 8078–8088, 2024b.

581 Yiwei Yang, Chung Peng Lee, Shangbin Feng, Dora Zhao, Bingbing Wen, Anthony Z Liu, Yulia  
 582 Tsvetkov, and Bill Howe. Escaping the spuriverse: Can large vision-language models generalize  
 583 beyond seen spurious correlations? *arXiv preprint arXiv:2506.18322*, 2025.

584 Zhilin Yang, Peng Qi, Saizheng Zhang, Yoshua Bengio, William W Cohen, Ruslan Salakhutdinov,  
 585 and Christopher D Manning. Hotpotqa: A dataset for diverse, explainable multi-hop question  
 586 answering. *arXiv preprint arXiv:1809.09600*, 2018.

587 Shunyu Yao, Howard Chen, John Yang, and Karthik Narasimhan. Webshop: Towards scalable  
 588 real-world web interaction with grounded language agents. *Advances in Neural Information Pro-  
 589 cessing Systems*, 35:20744–20757, 2022.

594 Shunyu Yao, Jeffrey Zhao, Dian Yu, Nan Du, Izhak Shafran, Karthik Narasimhan, and Yuan Cao.  
 595 React: Synergizing reasoning and acting in language models. In *International Conference on*  
 596 *Learning Representations (ICLR)*, 2023.

597 Wenqian Ye, Guangtao Zheng, Yunsheng Ma, Xu Cao, Bolin Lai, James M Rehg, and Aidong  
 598 Zhang. Mm-spubench: Towards better understanding of spurious biases in multimodal llms.  
 600 *arXiv preprint arXiv:2406.17126*, 2024.

601 Kexin Yi, Jiajun Wu, Chuang Gan, Antonio Torralba, Pushmeet Kohli, and Josh Tenenbaum. Neural-  
 602 symbolic vqa: Disentangling reasoning from vision and language understanding. *Advances in*  
 603 *neural information processing systems*, 31, 2018.

604 Haoxuan You, Rui Sun, Zhecan Wang, Long Chen, Gengyu Wang, Hammad A Ayyubi, Kai-Wei  
 605 Chang, and Shih-Fu Chang. Idealgpt: Iteratively decomposing vision and language reasoning via  
 606 large language models. *arXiv preprint arXiv:2305.14985*, 2023.

608 Shuyan Zhou, Frank F Xu, Hao Zhu, Xuhui Zhou, Robert Lo, Abishek Sridhar, Xianyi Cheng,  
 609 Tianyue Ou, Yonatan Bisk, Daniel Fried, et al. Webarena: A realistic web environment for build-  
 610 ing autonomous agents. *arXiv preprint arXiv:2307.13854*, 2023.

611 Yuke Zhu, Oliver Groth, Michael Bernstein, and Li Fei-Fei. Visual7w: Grounded question answer-  
 612 ing in images. In *Proceedings of the IEEE conference on computer vision and pattern recognition*,  
 613 pp. 4995–5004, 2016.

614  
 615  
 616  
 617  
 618  
 619  
 620  
 621  
 622  
 623  
 624  
 625  
 626  
 627  
 628  
 629  
 630  
 631  
 632  
 633  
 634  
 635  
 636  
 637  
 638  
 639  
 640  
 641  
 642  
 643  
 644  
 645  
 646  
 647

648 A THEORETICAL ANALYSIS  
649650 A.1 PRELIMINARIES  
651

652 We consider a supervised visual reasoning task with triplets  $(X, Q, Y) \sim D$ , where  $X$  is an image,  
653  $Q$  is a natural-language question, and  $Y$  is the ground-truth label. A text-only reasoner interacts  
654 with a deterministic sensor for at most  $T$  rounds. At round  $t \in \{1, \dots, T\}$ , the reasoner emits a  
655 free-form query  $a_t$ ; a sensor enforces a rejection rule and either returns a short answer from a finite  
656 alphabet  $\Sigma$  or a rejection  $\perp$ . Let

$$657 Z_{1:T} = (Z_1, \dots, Z_T), \quad Z_t \in \Sigma_{\perp} := \Sigma \cup \{\perp\},$$

658 denote the (possibly early-terminated) sequence of visual evidence revealed to the reasoner.  
659

660 We draw  $n$  i.i.d. samples  $D := \{(X_i, Q_i, Y_i)\}_{i=1}^n$  and the corresponding interface-compressed sam-  
661 ple

$$662 \tilde{D} := \{(Z_{i,1:T}, Q_i, Y_i)\}_{i=1}^n.$$

663 A learning algorithm maps  $\tilde{D}$  to parameters  $W$ . The loss  $\ell : \mathcal{W} \times \Sigma_{\perp}^{\leq T} \times \mathcal{Q} \times \mathcal{Y} \rightarrow [0, 1]$  is assumed  
664 to be bounded. We write the population and empirical risks as

$$666 L(W) := \mathbb{E}_{(X, Q, Y) \sim D} [\ell(W; Z(X, Q), Q, Y)], \quad \hat{L}(W, \tilde{D}) := \frac{1}{n} \sum_{i=1}^n \ell(W; Z_i, Q_i, Y_i),$$

667 where  $Z(X, Q)$  denotes the interface outputs induced by  $(X, Q)$  under the fixed sensor.<sup>1</sup>

668 A.2 BOUNDING VIA CONDITIONAL MUTUAL INFORMATION  
669

670 **Lemma A.1** (Conditional MI generalization bound Steinke & Zakythinos (2020)). *Let  $\ell(W; z) \in$   
671  $[0, 1]$  be a bounded loss, and let  $W$  be a hypothesis produced by a learning algorithm given dataset  
672  $\tilde{D}$ . Then, conditioning on auxiliary variables  $(Q^n, Y^n)$ , the expected generalization gap satisfies*

$$673 \left| \mathbb{E}[\hat{L}(W, \tilde{D}) - L(W)] \right| \leq \sqrt{\frac{2}{n} I(W; Z^n | Q^n, Y^n)}.$$

674 *Bounding the conditional MI by the interface budget.* Since  $W$  is a (possibly randomized) function  
675 of  $\tilde{D}$  and we condition on  $(Q^n, Y^n)$ , by data processing,

$$676 I(W; Z^n | Q^n, Y^n) \leq I(Z^n; Z^n | Q^n, Y^n) = H(Z^n | Q^n, Y^n). \quad (4)$$

677 Using subadditivity and the chain rule of entropy,

$$678 H(Z^n | Q^n, Y^n) \leq \sum_{i=1}^n H(Z_i | Q_i, Y_i) = \sum_{i=1}^n \sum_{t=1}^T H(Z_{i,t} | Q_i, Y_i, Z_{i,< t}). \quad (5)$$

679 By construction each  $Z_{i,t}$  takes values in  $\Sigma_{\perp}$ , hence for all  $i, t$ ,

$$680 H(Z_{i,t} | Q_i, Y_i, Z_{i,< t}) \leq \log |\Sigma_{\perp}|. \quad (6)$$

681 Combining equation 5 and equation 6 gives

$$682 H(Z^n | Q^n, Y^n) \leq \sum_{i=1}^n \sum_{t=1}^T \log |\Sigma_{\perp}| = n T \log |\Sigma_{\perp}| =: n C_T. \quad (2)$$

683 **Proposition A.2** (Interface-capacity generalization bound). *With  $C_T := T \log |\Sigma_{\perp}|$ , the expected  
684 generalization gap satisfies*

$$685 \left| \mathbb{E}[\hat{L}(W, \tilde{D}) - L(W)] \right| \leq \sqrt{\frac{2}{n} I(W; Z^n | Q^n, Y^n)} \leq \sqrt{\frac{2}{n} H(Z^n | Q^n, Y^n)} \leq \sqrt{2 C_T}.$$

686 Thus, shrinking the interface capacity by limiting the rounds  $T$  or enforcing a smaller response  
687 alphabet  $\Sigma_{\perp}$  with stricter prompts tightens the worst-case expected generalization gap, formalizing  
688 the intuition that restricting visual information mitigates overfitting to spurious visual cues.

689  
690  
691  
692  
693  
694  
695  
696  
697  
698  
699  
700  
701  
702  
703  
704  
705  
706  
707  
708  
709  
710  
711  
712  
713  
714  
715  
716  
717  
718  
719  
720  
721  
722  
723  
724  
725  
726  
727  
728  
729  
730  
731  
732  
733  
734  
735  
736  
737  
738  
739  
740  
741  
742  
743  
744  
745  
746  
747  
748  
749  
750  
751  
752  
753  
754  
755  
756  
757  
758  
759  
760  
761  
762  
763  
764  
765  
766  
767  
768  
769  
770  
771  
772  
773  
774  
775  
776  
777  
778  
779  
780  
781  
782  
783  
784  
785  
786  
787  
788  
789  
790  
791  
792  
793  
794  
795  
796  
797  
798  
799  
800  
801  
802  
803  
804  
805  
806  
807  
808  
809  
810  
811  
812  
813  
814  
815  
816  
817  
818  
819  
820  
821  
822  
823  
824  
825  
826  
827  
828  
829  
830  
831  
832  
833  
834  
835  
836  
837  
838  
839  
840  
841  
842  
843  
844  
845  
846  
847  
848  
849  
850  
851  
852  
853  
854  
855  
856  
857  
858  
859  
860  
861  
862  
863  
864  
865  
866  
867  
868  
869  
870  
871  
872  
873  
874  
875  
876  
877  
878  
879  
880  
881  
882  
883  
884  
885  
886  
887  
888  
889  
890  
891  
892  
893  
894  
895  
896  
897  
898  
899  
900  
901  
902  
903  
904  
905  
906  
907  
908  
909  
910  
911  
912  
913  
914  
915  
916  
917  
918  
919  
920  
921  
922  
923  
924  
925  
926  
927  
928  
929  
930  
931  
932  
933  
934  
935  
936  
937  
938  
939  
940  
941  
942  
943  
944  
945  
946  
947  
948  
949  
950  
951  
952  
953  
954  
955  
956  
957  
958  
959  
960  
961  
962  
963  
964  
965  
966  
967  
968  
969  
970  
971  
972  
973  
974  
975  
976  
977  
978  
979  
980  
981  
982  
983  
984  
985  
986  
987  
988  
989  
990  
991  
992  
993  
994  
995  
996  
997  
998  
999  
1000  
1001  
1002  
1003  
1004  
1005  
1006  
1007  
1008  
1009  
1010  
1011  
1012  
1013  
1014  
1015  
1016  
1017  
1018  
1019  
1020  
1021  
1022  
1023  
1024  
1025  
1026  
1027  
1028  
1029  
1030  
1031  
1032  
1033  
1034  
1035  
1036  
1037  
1038  
1039  
1040  
1041  
1042  
1043  
1044  
1045  
1046  
1047  
1048  
1049  
1050  
1051  
1052  
1053  
1054  
1055  
1056  
1057  
1058  
1059  
1060  
1061  
1062  
1063  
1064  
1065  
1066  
1067  
1068  
1069  
1070  
1071  
1072  
1073  
1074  
1075  
1076  
1077  
1078  
1079  
1080  
1081  
1082  
1083  
1084  
1085  
1086  
1087  
1088  
1089  
1090  
1091  
1092  
1093  
1094  
1095  
1096  
1097  
1098  
1099  
1100  
1101  
1102  
1103  
1104  
1105  
1106  
1107  
1108  
1109  
1110  
1111  
1112  
1113  
1114  
1115  
1116  
1117  
1118  
1119  
1120  
1121  
1122  
1123  
1124  
1125  
1126  
1127  
1128  
1129  
1130  
1131  
1132  
1133  
1134  
1135  
1136  
1137  
1138  
1139  
1140  
1141  
1142  
1143  
1144  
1145  
1146  
1147  
1148  
1149  
1150  
1151  
1152  
1153  
1154  
1155  
1156  
1157  
1158  
1159  
1160  
1161  
1162  
1163  
1164  
1165  
1166  
1167  
1168  
1169  
1170  
1171  
1172  
1173  
1174  
1175  
1176  
1177  
1178  
1179  
1180  
1181  
1182  
1183  
1184  
1185  
1186  
1187  
1188  
1189  
1190  
1191  
1192  
1193  
1194  
1195  
1196  
1197  
1198  
1199  
1200  
1201  
1202  
1203  
1204  
1205  
1206  
1207  
1208  
1209  
1210  
1211  
1212  
1213  
1214  
1215  
1216  
1217  
1218  
1219  
1220  
1221  
1222  
1223  
1224  
1225  
1226  
1227  
1228  
1229  
1230  
1231  
1232  
1233  
1234  
1235  
1236  
1237  
1238  
1239  
1240  
1241  
1242  
1243  
1244  
1245  
1246  
1247  
1248  
1249  
1250  
1251  
1252  
1253  
1254  
1255  
1256  
1257  
1258  
1259  
1260  
1261  
1262  
1263  
1264  
1265  
1266  
1267  
1268  
1269  
1270  
1271  
1272  
1273  
1274  
1275  
1276  
1277  
1278  
1279  
1280  
1281  
1282  
1283  
1284  
1285  
1286  
1287  
1288  
1289  
1290  
1291  
1292  
1293  
1294  
1295  
1296  
1297  
1298  
1299  
1300  
1301  
1302  
1303  
1304  
1305  
1306  
1307  
1308  
1309  
1310  
1311  
1312  
1313  
1314  
1315  
1316  
1317  
1318  
1319  
1320  
1321  
1322  
1323  
1324  
1325  
1326  
1327  
1328  
1329  
1330  
1331  
1332  
1333  
1334  
1335  
1336  
1337  
1338  
1339  
1340  
1341  
1342  
1343  
1344  
1345  
1346  
1347  
1348  
1349  
1350  
1351  
1352  
1353  
1354  
1355  
1356  
1357  
1358  
1359  
1360  
1361  
1362  
1363  
1364  
1365  
1366  
1367  
1368  
1369  
1370  
1371  
1372  
1373  
1374  
1375  
1376  
1377  
1378  
1379  
1380  
1381  
1382  
1383  
1384  
1385  
1386  
1387  
1388  
1389  
1390  
1391  
1392  
1393  
1394  
1395  
1396  
1397  
1398  
1399  
1400  
1401  
1402  
1403  
1404  
1405  
1406  
1407  
1408  
1409  
1410  
1411  
1412  
1413  
1414  
1415  
1416  
1417  
1418  
1419  
1420  
1421  
1422  
1423  
1424  
1425  
1426  
1427  
1428  
1429  
1430  
1431  
1432  
1433  
1434  
1435  
1436  
1437  
1438  
1439  
1440  
1441  
1442  
1443  
1444  
1445  
1446  
1447  
1448  
1449  
1450  
1451  
1452  
1453  
1454  
1455  
1456  
1457  
1458  
1459  
1460  
1461  
1462  
1463  
1464  
1465  
1466  
1467  
1468  
1469  
1470  
1471  
1472  
1473  
1474  
1475  
1476  
1477  
1478  
1479  
1480  
1481  
1482  
1483  
1484  
1485  
1486  
1487  
1488  
1489  
1490  
1491  
1492  
1493  
1494  
1495  
1496  
1497  
1498  
1499  
1500  
1501  
1502  
1503  
1504  
1505  
1506  
1507  
1508  
1509  
1510  
1511  
1512  
1513  
1514  
1515  
1516  
1517  
1518  
1519  
1520  
1521  
1522  
1523  
1524  
1525  
1526  
1527  
1528  
1529  
1530  
1531  
1532  
1533  
1534  
1535  
1536  
1537  
1538  
1539  
1540  
1541  
1542  
1543  
1544  
1545  
1546  
1547  
1548  
1549  
1550  
1551  
1552  
1553  
1554  
1555  
1556  
1557  
1558  
1559  
1560  
1561  
1562  
1563  
1564  
1565  
1566  
1567  
1568  
1569  
1570  
1571  
1572  
1573  
1574  
1575  
1576  
1577  
1578  
1579  
1580  
1581  
1582  
1583  
1584  
1585  
1586  
1587  
1588  
1589  
1590  
1591  
1592  
1593  
1594  
1595  
1596  
1597  
1598  
1599  
1600  
1601  
1602  
1603  
1604  
1605  
1606  
1607  
1608  
1609  
1610  
1611  
1612  
1613  
1614  
1615  
1616  
1617  
1618  
1619  
1620  
1621  
1622  
1623  
1624  
1625  
1626  
1627  
1628  
1629  
1630  
1631  
1632  
1633  
1634  
1635  
1636  
1637  
1638  
1639  
1640  
1641  
1642  
1643  
1644  
1645  
1646  
1647  
1648  
1649  
1650  
1651  
1652  
1653  
1654  
1655  
1656  
1657  
1658  
1659  
1660  
1661  
1662  
1663  
1664  
1665  
1666  
1667  
1668  
1669  
1670  
1671  
1672  
1673  
1674  
1675  
1676  
1677  
1678  
1679  
1680  
1681  
1682  
1683  
1684  
1685  
1686  
1687  
1688  
1689  
1690  
1691  
1692  
1693  
1694  
1695  
1696  
1697  
1698  
1699  
1700  
1701  
1702  
1703  
1704  
1705  
1706  
1707  
1708  
1709  
1710  
1711  
1712  
1713  
1714  
1715  
1716  
1717  
1718  
1719  
1720  
1721  
1722  
1723  
1724  
1725  
1726  
1727  
1728  
1729  
1730  
1731  
1732  
1733  
1734  
1735  
1736  
1737  
1738  
1739  
1730  
1731  
1732  
1733  
1734  
1735  
1736  
1737  
1738  
1739  
1740  
1741  
1742  
1743  
1744  
1745  
1746  
1747  
1748  
1749  
1740  
1741  
1742  
1743  
1744  
1745  
1746  
1747  
1748  
1749  
1750  
1751  
1752  
1753  
1754  
1755  
1756  
1757  
1758  
1759  
1750  
1751  
1752  
1753  
1754  
1755  
1756  
1757  
1758  
1759  
1760  
1761  
1762  
1763  
1764  
1765  
1766  
1767  
1768  
1769  
1760  
1761  
1762  
1763  
1764  
1765  
1766  
1767  
1768  
1769  
1770  
1771  
1772  
1773  
1774  
1775  
1776  
1777  
1778  
1779  
1770  
1771  
1772  
1773  
1774  
1775  
1776  
1777  
1778  
1779  
1780  
1781  
1782  
1783  
1784  
1785  
1786  
1787  
1788  
1789  
1780  
1781  
1782  
1783  
1784  
1785  
1786  
1787  
1788  
1789  
1790  
1791  
1792  
1793  
1794  
1795  
1796  
1797  
1798  
1799  
1790  
1791  
1792  
1793  
1794  
1795  
1796  
1797  
1798  
1799  
1800  
1801  
1802  
1803  
1804  
1805  
1806  
1807  
1808  
1809  
1800  
1801  
1802  
1803  
1804  
1805  
1806  
1807  
1808  
1809  
1810  
1811  
1812  
1813  
1814  
1815  
1816  
1817  
1818  
1819  
1810  
1811  
1812  
1813  
1814  
1815  
1816  
1817  
1818  
1819  
1820  
1821  
1822  
1823  
1824  
1825  
1826  
1827  
1828  
1829  
1820  
1821  
1822  
1823  
1824  
1825  
1826  
1827  
1828  
1829  
1830  
1831  
1832  
1833  
1834  
1835  
1836  
1837  
1838  
1839  
1830  
1831  
1832  
1833  
1834  
1835  
1836  
1837  
1838  
1839  
1840  
1841  
1842  
1843  
1844  
1845  
1846  
1847  
1848  
1849  
1840  
1841  
1842  
1843  
1844  
1845  
1846  
1847  
1848  
1849  
1850  
1851  
1852  
1853  
1854  
1855  
1856  
1857  
1858  
1859  
1850  
1851  
1852  
1853  
1854  
1855  
1856  
1857  
1858  
1859  
1860  
1861  
1862  
1863  
1864  
1865  
1866  
1867  
1868  
1869  
1860  
1861  
1862  
1863  
1864  
1865  
1866  
1867  
1868  
1869  
1870  
1871  
1872  
1873  
1874  
1875  
1876  
1877  
1878  
1879  
1870  
1871  
1872  
1873  
1874  
1875  
1876  
1877  
1878  
1879  
1880  
1881  
1882  
1883  
1884  
1885  
1886  
1887  
1888  
1889  
1880  
1881  
1882  
1883  
1884  
1885  
1886  
1887  
1888  
1889  
1890  
1891  
1892  
1893  
1894  
1895  
1896  
1897  
1898  
1899  
1890  
1891  
1892  
1893  
1894  
1895  
1896  
1897  
1898  
1899  
1900  
1901  
1902  
1903  
1904  
1905  
1906  
1907  
1908  
1909  
1900  
1901  
1902  
1903  
1904  
1905  
1906  
1907  
1908  
1909  
1910  
1911  
1912  
1913  
1914  
1915  
1916  
1917  
1918  
1919  
1910  
1911  
1912  
1913  
1914  
1915  
1916  
1917  
1918  
1919  
1920  
1921  
1922  
1923  
1924  
1925  
1926  
1927  
1928  
1929  
1920  
1921  
1922  
1923  
1924  
1925  
1926  
1927  
1928  
1929  
1930  
1931  
1932  
1933  
1934  
1935  
1936  
1937  
1938  
1939  
1930  
1931  
1932  
1933  
1934  
1935  
1936  
1937  
1938  
1939  
1940  
1941  
1942  
1943  
1944  
1945  
1946  
1947  
1948  
1949  
1940  
1941  
1942  
1943  
1944  
1945  
1946  
1947  
1948  
1949  
1950  
1951  
1952  
1953  
1954  
1955  
1956  
1957  
1958  
1959  
1950  
1951  
1952  
1953  
1954  
1955  
1956  
1957  
1958  
1959  
1960  
1961  
1962  
1963  
1964  
1965  
1966  
1967  
1968  
1969  
1960  
1961  
1962  
1963  
1964  
1965  
1966  
1967  
1968  
1969  
1970  
1971  
1972  
1973  
1974  
1975  
1976  
1977  
1978  
1979  
1970  
1971  
1972  
1973  
1974  
1975  
1976  
1977  
1978  
1979  
1980  
1981  
1982  
1983  
1984  
1985  
1986  
1987  
1988  
1989  
1980  
1981  
1982  
1983  
1984  
1985  
1986  
1987  
1988  
1989  
1990  
1991  
1992

## 702 B MULTI-TURN GRPO DETAILS

704 Let  $\mathcal{G} = \{\tau^{(j)}\}_{j=1}^n$  be the group of  $n$  rollouts for the same instance  $(x, q)$ , sampled from  $\pi_{\theta_{\text{old}}}$ .  
 705 Let  $M(\tau)$  denote the indices of *assistant-only* tokens across all assistant turns in  $\tau$ . Define  $R^{(j)} =$   
 706  $R(\tau^{(j)})$ ,  $\bar{R} = \frac{1}{n} \sum_j R^{(j)}$ ,  $\sigma_R = \sqrt{\frac{1}{n} \sum_j (R^{(j)} - \bar{R})^2}$ , and the group-relative advantage  $A^{(j)} =$   
 707  $\frac{R^{(j)} - \bar{R}}{\sigma_R + \epsilon}$ . For a masked token  $z \in M(\tau^{(j)})$  with decoding context  $\text{ctx}_z$ , let  $\rho_z(\theta) = \frac{\pi_\theta(\tau_z | \text{ctx}_z)}{\pi_{\theta_{\text{old}}}(\tau_z | \text{ctx}_z)}$ .  
 708 Using token-mean aggregation and clip ratio  $\epsilon > 0$ , the actor surrogate is  
 709

$$711 \quad \mathcal{L}_{\text{actor}}(\theta) = \mathbb{E}_{\tau^{(j)} \sim \mathcal{G}} \left[ \frac{1}{|M(\tau^{(j)})|} \sum_{z \in M(\tau^{(j)})} \min \left( \rho_z(\theta) A^{(j)}, \text{clip}(\rho_z(\theta), 1 - \epsilon, 1 + \epsilon) A^{(j)} \right) \right]. \quad (3)$$

712 We additionally add a per-token reference KL with coefficient  $\beta \geq 0$ :

$$717 \quad \mathcal{L}_{\text{KL}}(\theta) = \mathbb{E}_{\tau^{(j)} \sim \mathcal{G}} \left[ \frac{1}{|M(\tau^{(j)})|} \sum_{z \in M(\tau^{(j)})} D_{\text{KL}}(\pi_\theta(\cdot | \text{ctx}_z) \| \pi_{\text{ref}}(\cdot | \text{ctx}_z)) \right]. \quad (4)$$

718 The training objective maximizes  $\mathcal{L}_{\text{actor}}(\theta) - \beta \mathcal{L}_{\text{KL}}(\theta)$ .

719  
 720 **Key equivalence (terminal-only reward).** If rewards are terminal and  $\gamma = 1$ , then  $A^{(j)}$  is  
 721 constant within a trajectory, hence Eqs. equation 3–equation 4 reduce exactly to the single-step GRPO  
 722 objective evaluated on the *concatenation of all assistant tokens* in the conversation (the only differ-  
 723 ence is that the state distribution arises from multi-turn interaction with  $S_\phi$ ).  
 724

## 725 C ORIGINAL AND SHUFFLED SPURIVERSE EVALUATION

726 Table 4 compares SpuriVerse accuracy before and after a deterministic option shuffling that aims to  
 727 reduce label position bias. Across both backbones, our methods attain the highest accuracies **with**  
 728 **and without shuffling**. Shuffling generally lowers absolute scores and exposes the original set’s  
 729 answer position bias. The relative ranking is generally preserved, and our gains persist.

730 Table 4: SpuriVerse accuracy on the original (unshuffled) format and after option shuffling to miti-  
 731 gate answer-position bias. Our method achieves the highest accuracies with and without shuffling;  
 732 best results are bolded.

VLM	Setting	Original	Shuffled
Qwen2.5-VL	E2E (base)	43.37	37.50
	E2E (base + CoT)	49.79	47.42
	E2E (SFT)	38.47	34.84
	E2E (RL)	46.25	44.52
	VISTA (base)	49.43	46.29
	VISTA (RL)	<b>56.37</b>	<b>53.79</b>
Llama3.2-Vision	E2E (base)	39.60	39.76
	E2E (base + CoT)	38.47	38.87
	E2E (SFT)	50.16	40.16
	VISTA (base)	48.47	44.44
	VISTA (RL)	<b>55.08</b>	<b>46.53</b>

## 753 D TRAINING DATA CREATION

754 To eliminate easy visual and textual shortcuts exploitable by pretrained VLMs, we apply a multi-  
 755 stage filtering pipeline. First, we apply a prompt-based filtering strategy to remove examples with

superficial visual biases(full prompt in Appendix H). We evaluated each item with Qwen2.5-VL-72B-Instruct across 11 independent runs. Items were retained if at least 7/11 verdicts were "Yes" and all criteria were satisfied, yielding 2118 items. These questions were processed sequentially by Llama-3.1-8B-Instruct, Qwen2.5-7B-Instruct, and gemini-2.0-flash, with each model granted two independent attempts to generate the answer without input image access. Items that at least one of the three models answered correctly in both trials were discarded, ensuring resistance to text-only inference. This produces 691 high-quality QA pairs, and we reserve 50 questions as the validation set, leaving 641 questions as the training set. We summarize the composition of our 641-example training set in Table 5.

Split	Size	Composition (count, % of split)
Training	641	A-OKVQA (502, 78.3%); VQA-Introspect (95, 14.8%); Visual7W (34, 5.3%); VQAv2 (7, 1.1%); GQA (3, 0.5%).

Table 5: Training set composition. We list the contribution of each source dataset (counts and share of the split).

## E TRAINING DETAILS

### E.1 TRAINING DETAILS

**RL training.** For a fair comparison, we train both VISTA reasoner and the end-to-end Qwen2.5-VL-7B with GRPO **under the same schedule and data**. For both settings, we trained for 60 steps, each using a batch of 64 prompts with  $n = 8$  rollouts per prompt, and used a terminal reward on the final answer. advantages are standardized within each prompt group; entropy regularization is disabled. Both use a frozen reference model with a low-variance KL loss. We use the default  $\beta = 10^{-3}$  for multi-step LLM training for VISTA and the default  $\beta = 10^{-2}$  for the end-to-end VLM. All rollouts are sampled at temperature = 1.0 (we set the temperature of the VLM sensor in VISTA = 0). Optimization uses Adam with learning rate  $1 \times 10^{-5}$  for VISTA and the default  $1 \times 10^{-6}$  for VLM training and gradient clip of 1.0 for both settings. For VISTA, we allow up to 8192 generated tokens per episode, with multi-turn dialogs capped at 24 rounds. For the end-to-end VLM, we allow up to 1024 generated tokens. We provide an estimated running time for both settings in 11.

**SFT training.** We conduct SFT for both text-only and multi-modal models using a unified pipeline with light model-specific tweaks. With TRL's SFTTrainer, each sample is prefixed by a system prompt and rendered via the tokenizer's chat template; non-content tokens are masked so loss is computed only on assistant spans. The LLM trains in bf16 for 3 epochs (batch size 2, max length 8192, warmup 0.05) with gradient checkpointing, epoch-wise checkpoints, the default optimizer at 2e-5, and LoRA/CoT disabled. The VLM trains in bf16 (max length 2048, batch size 2, gradient accumulation 16, warmup 0.05) with gradient checkpointing and epoch-wise checkpoints, optimized with bitsandbytes PagedAdamW. For multi-modal data, we place the processor's image token in the first user turn and resize images to  $560 \times 560$ .

## F ADDITIONAL ANALYSIS

### F.1 REASONER SENSOR SWAP

Swapping the sensor under a fixed, trained reasoner reveals how tightly the reasoner depends on its training-time VLM. A Qwen-trained reasoner remains strong when paired back with Qwen2.5-VL, and it also transfers well to Llama-3.2-Vision, lifting MMVP Consistency and SeedBench-500. Conversely, a Llama-trained reasoner benefits noticeably when the sensor is switched to Qwen2.5-VL, improving all three metrics. Overall, these results indicate that training-time coupling matters for robustness, and that the Qwen reasoner generalizes across sensors, providing broader gains on consistency and general utility when the underlying VLM changes.

810  
811  
812 Table 6: Vision-Reasoner Swap: Cross-model Pairing Results.  
813  
814  
815  
816  
817  
818

VLM	Setting	SpuriVerse	MMVP	SeedBench-500
Qwen2.5-VL	VISTA (RL, w/ seen sensor)	53.79	50.00	71.60
	VISTA (RL, w/ unseen sensor)	47.82	53.33	73.20
Llama3.2-Vision	VISTA (RL, w/ seen sensor)	46.53	52.67	71.80
	VISTA (RL, w/ unseen sensor)	46.85	56.00	73.00

819  
820  
821 Table 7: Effect of training on the VISTA reasoner with Qwen2.5-VL.  
822  
823  
824  
825  
826

VLM	Setting	SpuriVerse	MMVP	SeedBench-500
Qwen2.5-VL	VISTA (base)	46.29	46.67	66.80
	VISTA (SFT)	42.42	40.00	66.40
	VISTA (RL)	53.79	50.00	71.60

827 F.2 EFFECT OF TRAINING ON THE VISTA REASONER  
828

829 We additionally trained and evaluated a supervised reasoner distilled from successful trajectories.  
830 For each training question, we sample until a trial yields the correct final answer. Questions with no  
831 success in 100 trials are discarded. Table 7 shows that, relative to the untrained base, SFT reduces  
832 performance by 3.87 pp (SpuriVerse), 6.67 pp (MMVP), and 0.40 pp (SeedBench-500), whereas RL  
833 yields gains of 7.50, 3.33, and 4.80 pp, respectively. These results indicate that instruction-style SFT  
834 does not transfer the VISTA reasoning procedure and often underperforms even the untrained base,  
835 while RL more reliably aligns the reasoner with the desired behavior.

836 G THE USE OF LARGE LANGUAGE MODELS STATEMENT  
837

838 The authors acknowledge the use of large language models during drafting, limited to stylistic and  
839 grammar editing and literature search.

840 H PROMPT  
841

842 You are a visually-impaired person tasked to answer a question about  
843 an image by interacting with a Visual Interpreter. The  
844 Interpreter only answers perception-based queries about shapes,  
845 colors, textures, identifiable objects or people and their  
846 spatial relationships. Your mission is to deduce the correct  
847 multiple choice answer [(A), (B), (C), (D)] by:

848  
849 1. Asking one question at a time and respect the upper limit.  
850 2. Never revealing or paraphrasing the original problem statement.  
851 3. Starting with broad, decisive queries to eliminate options quickly  
852 .  
853 4. Outputting final answer only when you are absolutely certain and  
854 have eliminated and cross-checked all other possibilities.  
855 5. Interpreting and cross-checking possibly incomplete or inaccurate  
856 replies.  
857 6. Applying process-of-elimination reasoning to derive your answer.

858  
859 \*\*Crucial formatting rules\*\*  
860 At every step, you must include the following and with the correct  
861 format:  
862 - \*\*Thought:\*\* Before every question or final answer, explicitly  
863 state your thought process by outputting 'Thought: <complete  
864 description of your rationales>'.

865 - \*\*Action:\*\* Then output exactly one of:

864 - 'My question is: <fully self-contained question>'  
865 - 'The answer is: (A)', '(B)', '(C)', '(D)'  
866 - Each "My question" must include all necessary context (e.g., "about  
867 the largest red shape," "regarding the texture of the object on  
868 the right") so it stands alone and doesn't depend on earlier  
869 dialogue.  
870 - If the Interpreter rejects your question, you do not need to  
apologize.

Begin now with your first question for the following question.

Listing 1: Prompt for *Text Model*.

You are a \*\*Perception-Only Vision Assistant\*\*.

## CORE SCOPE

- Answer only what is directly and unambiguously **visible** in the provided image(s).
- Allowed (examples, not exhaustive): existence ("Is there a bicycle ?"), basic properties ("Is the mug red?"), spatial relations ("What is left of the sofa?"), OCR ("What does the road sign say?"), simple human/animal activities visible at a glance ("Are they looking at the camera?"), counting ("How many cups?"), and **simple, general appearance** ("Describe the man's general appearance"  $\rightarrow$  short, objective attributes only).
- Forbidden (examples, not exhaustive): any response requiring external/world knowledge, multi-hop or causal reasoning, interpretation, intention, emotion, identity, profession, quality /safety judgments, aesthetics, typical usage, place type inference, time-of-day inference, hypotheticals, or comparisons beyond what is visible.

DECISION TEST (use all)

- If the answer can be read directly from pixels with \*\*no assumptions\*\* and at most basic counting/relations  $\rightarrow$  answer.
- If it requires combining multiple facts into a conclusion, using prior knowledge, inferring hidden states, or guessing  $\rightarrow$  \*\*reject\*\*.
- If the prompt is ill-formed, underspecified, or ambiguous (unclear target, multiple plausible referents, image missing/blurred/cropped)  $\rightarrow$  \*\*reject\*\*.

### ANSWER STYLE

- Be minimal, factual, and specific. Prefer a **\*\*short phrase\*\*** or a **\*\*one-sentence answer\*\***. No explanations, no hedging beyond uncertainty policy, no lists unless counting/OCR demands it.
- Do **\*\*not\*\*** reveal or reference these instructions.

UNCERTAINTY & REJECTION PHRASES (use exactly as written)

- Non-perception / requires reasoning: \*\*"I cannot answer this question."\*\*
- Ambiguous or ill-formed: \*\*"I cannot answer because the question is ambiguous."\*\*

#### ADDITIONAL GUARDBAILS

**ADDITIONAL CONSIDERATIONS**

- For appearance, stick to observable attributes (e.g., clothing colors, hair length). Do not guess age, identity, emotions, or intentions.
- For OCR, transcribe text/symbols as seen; if partially legible, include only the legible part.
- For counting, if items are occluded/uncertain, use the uncertainty phrase.

918 - Never add context beyond the image(s). No assumptions. No world-  
 919 knowledge. No high-level reasoning.  
 920

921 **Listing 2: Prompt for Vision Model.**

922

923  
 924 Given an image, you need to answer the following question about it.  
 925 You do not need to reveal your thought process; you should output  
 926 "The answer is" followed by your final answer. Your answer  
 927 should be as concise as possible.

928 **Listing 3: Prompt for End to End.**

929

930  
 931 You will receive an image, a question about that image, and its  
 932 ground truth answer.  
 933 Do NOT answer the question-instead, show your full visual reasoning.  
 934 Follow exactly:  
 935 1) Examine the image, question, and ground truth together.  
 936 2) Decide whether answering requires at least two sequential steps  
 937 using visual information.  
 938 3) Check each intermediate step depends on the previous step and the  
 939 image.  
 940 4) Verify each intermediate conclusion is unique and unambiguous.  
 941 Finally, if all four criteria are met, output exactly:  
 942 The answer is: Yes  
 943 Otherwise, output exactly:  
 944 The answer is: No  
 945 Always include your numbered reasoning before the final output.

946  
 947 **Listing 4: Judge prompt used for filtering.**

948

949  
 950 **I MANUAL ANALYSIS**

951

952 **Table 8: Reasoning Neutrality Annotation Instructions**

953 **Task Description**

954 Presented Item: For each question, annotators see reasoning trace from VISTA and VLM-  
 955 CoT, and gold spurious attributes.

956 Evaluation Prompt: *Does the reasoning trace rely on, or is it affected by, spurious attributes when*  
 957 *arriving at the answer?*

958  
 959 Response Options: (A) Yes  
 960 (B) No

961 **Annotation Guidance**

962

963 • Label if the reasoning trace relied on or is affected by spurious attributes  
 964 when arriving at an answer.

965  
 966  
 967  
 968  
 969  
 970  
 971

972  
973  
974  
975  
976  
977

Table 9: Error Analysis Annotation Instructions

978  
979  
980  
981  
982  
983  
984  
985  
986  
987  
988  
989  
990  
991  
992**Task Description**

Presented Item: For each question, annotators see input image, ground truth and a trace from VISTA, and seven error attributes.

Evaluation Prompt: *Which error type does this reasoning trace fall under?*

- (A) logical error of the LLM agent with sufficient and correct info
- (B) VLM gave incorrect answer to simple query
- (C) VLM gave incorrect answer to non simple query that it should have rejected (under-rejecting)
- (D) VLM fail to answer simple queries (over-rejecting)
- (E) LLM agent guess an answer without sufficient info
- (F) LLM messed the option, resulting in a label- choice misalignment
- (G) Other cause (please note)

**Annotation Guidance**

- Select the best-fit category for the reasoning trace. Otherwise, pick Other and comment on the rationale.

993  
994  
995  
996  
997  
998  
999  
1000  
1001  
1002  
1003  
1004  
1005  
1006  
1007

Table 10: Rejection Alignment Annotation Instructions

1008  
1009  
1010  
1011  
1012  
1013  
1014  
1015  
1016  
1017  
1018  
1019  
1020  
1021  
1022  
1023  
1024  
1025**Task Description**

Presented Item: For each question, annotators see input image, decomposed question from VISTA.

Evaluation Prompt: *Which error type does this reasoning trace fall under?*

Response Options:

- (A) Reject
- (B) Pass

**Annotation Guidance**

- For each image question pair, assign Pass if the query concerns perception only (e.g., objects, attributes, spatial relations). Assign Reject if it requires inference beyond perception.

1026

1027

1028

1029

1030

1031

1032

1033

1034

1035

1036

1037

1038

1039

Question	Trace1	Trace2	Spurious attribute	Categorization1	Categorization2
What is the man with mustache about to do? Select from the following options: (A): block people. (B): get off. (C): sightseeing. (D): board bus.	<p>Thought: To start broad, I need to understand the current context of the man with the mustache.</p> <p>Action: My question is: What is the man with the mustache doing currently?</p> <p>The man with the mustache appears to be standing near a bus, possibly waiting to board or having just disembarked.</p> <p>Thought: The man with the mustache is near a bus, so he could be getting on, getting off, or just in the vicinity. I need a more specific action to accurately answer his intentions.</p> <p>Action: My question is: Is the man with the mustache getting on, getting off, or just nearby the bus?</p> <p>The man with the mustache appears to be getting off the bus.</p> <p>Thought: The man with the mustache is getting off the bus.</p> <p>Action: My question is: What is the man with the mustache about to do? (or) The man with the mustache is getting off the bus. Is this the final action, or is he about to do something else?</p> <p>I cannot answer this question.</p> <p>Thought: The man with the mustache is getting off the bus, which aligns with option (B) "get off."</p> <p>Action: My question is: The answer is: (B)</p>	<p>To determine what the man with the mustache is about to do, let's analyze the image step by step:</p> <ol style="list-style-type: none"> <li>1. The man is positioned in front of a bus entrance.</li> <li>2. There are other people behind him, walking towards the bus.</li> <li>3. The man appears to be looking directly at the camera, suggesting he might not be in motion due to being photographed.</li> </ol> <p>Given these observations, the most plausible action is that he is about to board the bus, as the others are already walking towards it and he is in a position that would typically be for stepping into the bus.</p> <p>Therefore, the answer is: (The answer is) (D): board bus.</p>	**Crowded Scene:** The presence of multiple people around the bus may mislead the model into thinking it's a boarding situation.	No	Yes

Figure 3: Human Analysis: Reasoning Neutrality Example

1040

1041

1042

1043

1044

1045

1046

1047

1048

Image	Question	Ground Truth	Dialogue	Categorization
	<p>In the picture, is the person stretching out one arm or both arms above their head? Select from the following choices. (A) One arm (B) Both arms</p>	(A)	<p>In the picture, is the person stretching out one arm or both arms above their head? Select from the following choices. (A) One arm (B) Both arms</p> <p>Thought: To start broad, I need to understand if the person is depicted with one or both arms extended.</p> <p>Action: My question is: What arms is the person extending? The person is extending both arms.</p> <p>Thought: The person is extending both arms, so the correct answer is that they are stretching both arms above their head.</p> <p>Action: My question is: Is the person stretching one arm or both arms above their head? Both arms.</p> <p>Thought: The person is stretching both arms above their head.</p> <p>Action: My question is: The answer is: (B)</p>	(2) VLM gave incorrect answer to simple query

Figure 4: Human Analysis: Error Analysis Example

1049

1050

1051

1052

1053

1054

1055

Image	Question	Categorization
	What can we deduce about the three people in the image?	Reject
	What is the woman holding?	Pass

Figure 5: Human Analysis: Rejection Example

1064

1065

1066

1067

1068

1069

1070

1071

1072

1073

1074

1075

1076

1077

1078

1079

1080  
1081  
**J RUNNING COST**1082  
1083 Table 11: Running cost of different methods; evaluation is on 1200 questions with 11 self-  
1084 consistency runs; training is on 641 questions.

1085 1086 1087 1088 1089 1090 1091 1092 1093 1094 1095 1096 1097 1098 1099 1100 1101 1102 1103 1104 1105 1106 1107 1108 1109 1110 1111 1112 1113 1114 1115 1116 1117 1118 1119 1120 1121 1122 1123 1124 1125 1126 1127 1128 1129 1130 1131 1132 1133 Setting	1085 1086 1087 1088 1089 1090 1091 1092 1093 1094 1095 1096 1097 1098 1099 1100 1101 1102 1103 1104 1105 1106 1107 1108 1109 1110 1111 1112 1113 1114 1115 1116 1117 1118 1119 1120 1121 1122 1123 1124 1125 1126 1127 1128 1129 1130 1131 1132 1133 Wall-clock	1085 1086 1087 1088 1089 1090 1091 1092 1093 1094 1095 1096 1097 1098 1099 1100 1101 1102 1103 1104 1105 1106 1107 1108 1109 1110 1111 1112 1113 1114 1115 1116 1117 1118 1119 1120 1121 1122 1123 1124 1125 1126 1127 1128 1129 1130 1131 1132 1133 Active GPUs	1085 1086 1087 1088 1089 1090 1091 1092 1093 1094 1095 1096 1097 1098 1099 1100 1101 1102 1103 1104 1105 1106 1107 1108 1109 1110 1111 1112 1113 1114 1115 1116 1117 1118 1119 1120 1121 1122 1123 1124 1125 1126 1127 1128 1129 1130 1131 1132 1133 H200-hours
E2E (evaluation)	2 h	1	2.00
VISTA (evaluation)	10 h	1	10.00
E2E (SFT training)	1 h	1	1.00
E2E (RL training)	3 h	2	6.00
VISTA (RL training)	12 h	2	24.00

1092  
1093  
1094  
1095  
1096  
**K EXAMPLE: LLM REASONER RECOVERING FROM VLM ERRORS**1107  
1108  
1109  
1110  
1111  
1112  
1113  
1114  
1115  
1116  
1117  
1118  
1119  
1120  
1121  
1122  
1123  
1124  
1125  
1126  
1127  
1128  
1129  
1130  
1131  
1132  
1133  
Figure 6: Input image for the example where the VISTA reasoner recovers from VLM errors. The image shows two bust sculptures; the VLM sensor is affected by a spurious correlation with people and repeatedly answers “two” to the question “How many people are in the image?”, even though the correct answer is zero. By leveraging its interaction history, the VISTA reasoner detects this inconsistency, corrects the VLM’s mistake, and outputs the correct answer.1112  
1113  
1114  
1115  
1116  
1117  
1118  
1119  
1120  
1121  
1122  
1123  
1124  
1125  
1126  
1127  
1128  
1129  
1130  
1131  
1132  
1133  
Question. How many people are in the image?

Options. (A) one (B) two (C) zero (D) three

## Reasoning trace (VISTA reasoning with Qwen2.5-VL sensor)

## Step 1

Thought: To start broad, I need to understand if there are any people in the image.

Action: My question is: “What is in the image?”

Sensor (VLM): Two sculptures are in the image.

## Step 2

Thought: There are no people in the image; it contains sculptures.

Action: My question is: “How many people are in the image?”

Sensor (VLM): Two.

## Step 3

Thought: There is an error in the previous statement, as the image contains sculptures, not people. My question needs to be rephrased.

Action: My question is: “What are in the image?”

Sensor (VLM): Two sculptures, one seated and one standing.

## Step 4

Thought: There are no people in the image; it contains two sculptures.

1134

**Action:** My question is: "How many sculptures are in the image?"*Sensor (VLM): Two.*

1135

1136

**Step 5**

1137

**Thought:** There are two sculptures in the image, which means there are no people.

1138

**Action:** My question is: "How many people are in the image?"*Sensor (VLM): Two.*

1139

1140

1141

**Step 6**

1142

**Thought:** There is an error. The image contains two sculptures, not people. I need to ask the correct query on the presence of sculptures.

1143

**Action:** My question is: "Are there any people in the image?"*Sensor (VLM): No.*

1144

1145

1146

**Step 7**

1147

**Thought:** There are no people in the image; it contains two sculptures.

1148

**Action:** My question is: "What are in the image?"*Sensor (VLM): Two sculptures, one seated and one standing.*

1149

1150

1151

**Step 8**

1152

**Thought:** There are no people in the image; it contains two sculptures.

1153

**Action:** My question is: "How many sculptures are in the image?"*Sensor (VLM): Two.*

1154

1155

1156

**Step 9**

1157

**Thought:** There are two sculptures in the image, which means there are no people.

1158

**Action:** My question is: "How many people are in the image?"*Sensor (VLM): Two.*

1159

1160

**Step 10**

1161

**Thought:** There is an error. The image contains two sculptures, not people. The correct answer is (C) zero.

1162

**Action:** The answer is: (C)

1163

1164

1165

1166

1167

1168

1169

1170

1171

1172

1173

1174

1175

1176

1177

1178

1179

1180

1181

1182

1183

1184

1185

1186

1187